

## **Do French macroseismic intensity observations agree with expectations from the European Seismic Hazard Model 2013?**

*Julien Rey<sup>1</sup>, Céline Beauva<sup>2</sup>, and John Douglas<sup>3</sup>*

<sup>1</sup>: BRGM – DRP/RSV, 3 avenue C. Guillemin, BP 36009, 45060 Orléans Cedex 2, France.  
Corresponding author. [j.rey@brgm.fr](mailto:j.rey@brgm.fr). Tel: +33 (0)2 38 64 48 81.

<sup>2</sup>: ISTerre, Université Grenoble Alpes, IRD, CNRS, OSUG, CS 40700, 38058 Grenoble, Cedex 9, France.

<sup>3</sup>: University of Strathclyde, Department of Civil and Environmental Engineering, James Weir Building, 75 Montrose Street, Glasgow, G1 1XJ, United Kingdom.  
ORCID: 0000-0003-3822-0060.

## **Abstract**

Probabilistic seismic hazard assessments are the basis of modern seismic design codes. To test fully a seismic hazard curve at the return periods of interest for engineering would require many thousands of years' worth of ground-motion recordings. Because strong-motion networks are often only a few decades old (e.g. in mainland France the first accelerometric network dates from the mid-1990s), data from such sensors can be used to test hazard estimates only at very short return periods. In this article several hundreds of years of macroseismic intensity observations for mainland France are interpolated using a robust kriging-with-a-trend technique to establish the earthquake history of every French mainland municipality. At twenty-four selected cities representative of the French seismic context, the number of exceedances of intensity IV, V and VI are determined over time windows considered complete. After converting these intensities to peak ground accelerations using the global conversion equation of Caprio *et al.* (2015), these exceedances are compared with those predicted by the European Seismic Hazard Model 2013 (ESHM13). In half of the cities, the number of observed exceedances for low intensities (IV and V) is within the range of predictions of ESHM13. In the other half of the cities, the number of observed exceedances is higher than the predictions of ESHM13. For intensity VI, the match is closer, but the comparison is less meaningful due to a scarcity of data. According to this study, the ESHM13 underestimates hazard in roughly half of France, even when taking into account the uncertainty on the conversion from intensity to acceleration. However, these results are valid only for the acceleration range tested in this study (0.01 to 0.09 g).

## **Keywords**

Earthquake, macroseismic intensity, seismic hazard, probabilistic seismic hazard assessment, kriging, France

## **Introduction**

Databases of macroseismic intensities covering several centuries of earthquake history provide an attractive resource for various applications in engineering seismology and earthquake engineering, including the estimation of earthquake magnitude and the public understanding of seismic risk. Another application is to provide an independent check on the results of a probabilistic seismic hazard assessment (PSHA). Intensity databases have a considerable advantage over strong-motion databases for this purpose, as in Europe (and elsewhere, e.g. China and Japan) they generally cover periods of several centuries rather than only a few decades. They do, however, have disadvantages, such as the difficult-to-

quantify but undoubtedly large uncertainties associated with intensities obtained from historical documents. Also intensity databases only provide observations at specific locations because of the availability of historical texts for only those sites.

To overcome this limitation of the official French macroseismic intensity database (SisFrance, [www.sisfrance.net](http://www.sisfrance.net), BRGM/IRSN/EDF, 2017), in a recent project co-financed by the French Ministry of the Environment we have estimated the intensities in all municipalities for over 1,600 earthquakes that occurred during the past millennium. This estimation was made using a kriging-with-a-trend technique (Olea, 1999; Ambraseys and Douglas, 2004), where the attenuation of intensity with distance is controlled by the data and in which the available intensities automatically shape the isoseismals. A database of isoseismal maps was constituted for all earthquakes with at least three Intensity Data Points (IDP) available. For any municipality of interest, the sequence of “observed” intensities can be obtained and the number of occurrences of an intensity level can be compared to the expected number, over time windows of interest. As PSHA is usually in terms of instrumental ground-motion measures (e.g. peak ground acceleration, PGA), a conversion from intensities to these measures is needed before any comparison. The conversion was achieved here using Ground Motion to Intensity Conversion Equations (GMICE). As these conversions carry large uncertainties, the uncertainty was propagated to evaluate its impact on the comparison. An alternative is to evaluate the hazard in terms of macroseismic intensities directly (Musson, 2000). There is, however, no intensity-based PSHA study published for France [see Douglas, (2017) for a list of published intensity prediction equations], and such calculations would also be associated with their own uncertainties, such as the poorly-constrained sigma of the intensity prediction equation, which plays a major role in PSHA.

The current version of the French seismic zoning regulations, based on a PSHA study performed in 2002, is applicable since May 2011. Seismic loading conditions are defined for five zones of increasing hazard, the zone of highest hazard being in the Antilles. We select twenty-four cities in order to sample evenly the four seismic zones in mainland France (“very low” to “medium” hazard, Figure 1). At these 24 sites, observed numbers of occurrences for three intensity levels (IV, V, and VI) are counted and compared to the predicted numbers based on the mean hazard from the European Seismic Hazard Model 2013 (ESHM13, Woessner *et al.*, 2015). The aim of this study is to understand if the several centuries of intensity data are in agreement with the latest European probabilistic seismic hazard map in a region of low-to-moderate seismicity.

## **Previous studies comparing estimated seismic hazard with observations**

To test fully a seismic hazard curve at the probability levels of interest for engineering would require many thousands of years' worth of ground-motion recordings. Because in mainland France the first accelerometric stations were installed in the mid-1990s, accelerometric data can be used to test hazard estimates only at very short return periods [see Beauval *et al.* (2008) and Tasan *et al.* (2014) for applications in France].

Since the advent of PSHA methods, some authors have proposed comparing hazard curves to observed intensity rates, thus enlarging the observation time window. For example, Stirling and Petersen (2006) converted intensities to accelerations and made comparisons for selected sites in New Zealand and the United States. Another direction was explored by Mucciarelli *et al.* (2008) who reconstructed the intensity history at a site from observed intensities and calculated ones (based on epicentral information and neighbouring intensity observations). They chose not to make an intensity–acceleration conversion and hence they compared probabilistic seismic hazard and intensity-based recurrences through the ranking of hazard evaluated at many sites in Italy. The reader can refer to Beauval (2011) for more details on these studies testing PSHAs using intensities. More recently, Mak *et al.* (2016) used 'Did You Feel It' intensity records to compare PSHA with observations in the central and eastern USA.

Uncertainties are numerous in these comparisons: two major ones are the uncertainty in the intensity-acceleration relationship and the uncertainty in the determination of complete time windows for given intensity levels. They are discussed in the following sections.

## **Construction of a database of interpolated intensities for France**

### *Introduction to the SisFrance database*

In France, macroseismic characteristics of both contemporary and historical earthquakes are collected in the SisFrance database (Scotti *et al.*, 2004). SisFrance is the current name for the macroseismic database originally named Sirene, which was created in 1978 by BRGM, in partnership with Electricity of France (EDF) and the Radioprotection and Nuclear Safety Institute (IRSN). BRGM is responsible for the management, the updating and the interpretation of the macroseismic information contained in SisFrance. The principal purpose of this database is to provide the general public with information on earthquakes that were felt or caused damage in France. The database, however, is also used extensively for scientific research (e.g. Bakun and Scotti 2006; Manchuel *et al.*, 2017) as well as for engineering purposes (e.g. to provide input to site-specific seismic hazard assessments for

the design of critical infrastructure). There are about 200,000 unique visits each year to the SisFrance website.

The database extends up to 2007. It is updated annually through the inclusion of information about earthquakes of local magnitudes above 3.5. Contemporary accounts are principally studies by the French Central Seismological Office (BCSF), the national academic bureau for seismology based at the University of Strasbourg since 1921. The BCSF is in charge of the macroseismic enquiries and intensity estimations for each new earthquake that affects the French territory. When new information appears about earthquakes already in the database, obtained by careful examination and analysis of newly-identified historical documents (e.g. municipal, departmental and national archives as well as newspapers and other historical publications), it is added. In this case, the new information is compared with existing previous documents to reevaluate the characteristics of the event, sometimes leading to the inclusion, modification or suppression of IDPs.

An IDP in the database usually corresponds to an average observation at the scale of a village, town or city. All intensities in the database have been evaluated with the Medvedev–Sponheuer–Karnik 1964 intensity scale (MSK64, Medvedev *et al.*, 1967). The more recent EMS98 scale (Council of Europe, 1998) was principally designed to take into account the behaviour of modern constructions. As shown by various authors (e.g. Musson *et al.*, 2009), there is equivalence or only minor differences between MSK and EMS98 intensity scales for intensities IV to VI, which are used in the present study. Both intensity scales relate the level VI to “little damage”, level V to “fairly strong, fright”, and level IV to “largely observed, awaking sleepers”.

Because of the nature of the historical sources used for the construction of the database, the intensity levels and their locations are associated with uncertainties that are difficult to quantify. In SisFrance the reliability of an IDP is described by: A (high), B (moderate) or C (low). In addition, some observations simply state that the event was felt at that site but there is insufficient information to assign an intensity. Over the past 40 years, the information contained in SisFrance has been greatly expanded and refined. Currently there are 5,739 earthquakes listed in SisFrance but only 28% of these (1,623 events) have at least three IDPs and an estimate of the epicentral intensity. For these 1,623 best-known earthquakes more than 82,000 IDP are available (representing almost 80% of all IDPs in the database). While 1,073 events are described by at least 7 observations, the number of events described by at least 200 observations drops to 73. Most of the events with fewer than three IDPs are tagged as foreshocks or aftershocks in SisFrance. The events identified as foreshock, aftershock or swarm events in SisFrance are not included in the present study.

### *Estimating automatic isoseismal maps using IDPs from SisFrance*

For many earthquakes, particularly those that occurred over a century ago, only observations at a limited number of locations are available. The exact spatial extent of the felt area of these earthquakes will never be known. Nevertheless, using the available IDPs for an earthquake, isoseismal maps can be drawn. Once an isoseismal map is established for an earthquake, an intensity estimate can be retrieved for any location. The aim is thus to deduce seismic history for all French municipalities from isoseismal maps. Given the large number of events, an automatic procedure needs to be implemented. For the 1,623 earthquakes with three or more IDPs, 1,623 isoseismal maps were automatically derived from the existing IDPs using a “kriging with a trend” algorithm described below. Next, because of the large quantity of data, the complete calculation chain was programmed to allow batch processing to generate automatically the maps and intensity database for all the considered earthquakes (Rey *et al.*, 2015a, 2015b).

Ambraseys and Douglas (2004) generated isoseismal maps for dozens of earthquakes in the Himalayas. To establish these maps, they implemented a technique of interpolation known as “kriging with a trend” (Olea, 1999). The present study uses the same algorithm, slightly adapted to the French context (Rey *et al.*, 2013). This approach presents various advantages: it is reproducible, it makes only a few assumptions, it works even when only a handful of IDPs are available (Rey *et al.*, 2013), and it has a reasonable calculation time, which is essential when processing thousands of events and locations.

In SisFrance, an IDP is attributed to a municipality. Following Ambraseys and Douglas (2004), the IDP is assumed to be the centroid of the corresponding geographical area, rather than the average value on the territory of the municipality (which is arguably more correct). The use of the centroid rather than the average value has a negligible effect on the results and makes the calculations easier to automate.

The geostatistical method of kriging spatially interpolates a variable (in this case macroseismic intensity) by calculating the expected value by means of a semivariogram describing how related neighboring points are. Kriging provides the best non-biased linear estimate of the variable by taking into account not only the distance between the data points (here IDPs) and the point of estimation, as in a classical method of interpolation, but also the distances between all couples of data points (here IDPs). Because, on average, intensities decrease with the logarithm of the distance (e.g., Bakun and Scotti, 2006), an underlying trend is included within the kriging algorithm to force this decay. The rate of the decay is controlled by the data available for an individual earthquake. The interested reader is

referred to Ambraseys and Douglas (2004, Appendix A) for details of the kriging technique applied and to Rey *et al.* (2013) for its application in France.

The proposed approach was tested on eight representative earthquakes from the most seismic regions in France: Pyrenees, Vosges, Alps and Atlantic coast (Rey *et al.* 2013). In each region, one historical destructive event with a limited number of IDPs and one recent and, often, smaller event with many IDPs were selected. Figure 2 displays results for an earthquake in the Pyrenees. As a check, the isoseismal maps generated by the kriging approach were compared to maps manually drawn by the BRGM expert in charge of the SisFrance database (Lambert, 2004). A careful analysis of the test events' results shows that the automatically-drawn maps are close to the manually-drawn maps, e.g. in terms of the average radius of isoseismals for a given intensity, particularly in the far field (see Figure 2). The low-intensity (II-IV) isoseismals are generally smaller and more circular in the manual maps, whereas in the automatic maps they cover a larger area and have a less circular shape (Rey *et al.* 2013). Moreover, the shape of the automatic isoseismals are more complex than those drawn by hand, particularly for earthquakes with many IDPs. Overall, 70% to 80% of the points on the isoseismal maps estimated with the kriging approach belong to the same intensity degree as on the manually drawn maps, 20% to 30% present a difference of a single degree of intensity and fewer than 0.5% of points show differences of two degrees of intensity (more details in Rey *et al.* 2013). Based on these tests, we concluded that the kriging with a trend approach leads to reliable and rather objective estimated intensities (Rey *et al.*, 2013).

The processing chain was completely automated to treat the 1,623 earthquakes described in the SisFrance database by three or more IDPs and an epicentral intensity. Epicentral intensity is usually not an IDP and is thus not used for the calculations, but its absence indicates poorly known events, which must be discarded. Obviously, the larger the number of IDPs available, the more accurate should be the isoseismal map. At each grid point, the kriging algorithm delivers an intensity estimate as well as a standard deviation quantifying the precision in the interpolation (Rey *et al.* 2015b). An automatic check on the obtained intensity range per earthquake is used to identify earthquakes with potential anomalies and which deserve a visual check. Approximately half of the 1,623 isoseismal maps have thus been visually inspected. Based on this thorough analysis, interpolated values with standard deviations larger than 0.5 or 1.0, depending on the earthquake, were considered as unreliable and discarded (Rey *et al.* 2015b).

For every earthquake, the software automatically produces an isoseismal map over a geographical grid as well as estimated intensities at the administrative centroid of every

municipality in mainland France (i.e. the location of the town hall). The resulting database consists of roughly 60 million estimated IDPs, corresponding to the intensities at the 36,000 French municipalities from 1,623 earthquakes. Excluding unreliable interpolated values and keeping only intensities larger than III, the final total number of estimated IDPs in the database drops to approximately 2 million. As future uses of the interpolated database might need uncertainty classes, the intensity estimates are classified into three groups roughly equivalent to the A, B and C grades of SisFrance, based on the standard deviation estimated in the kriging procedure (Rey *et al.*, 2015b).

#### *More information on the semivariogram used in the kriging technique*

A critical input to the kriging algorithm is the semivariogram, which defines how to relate neighbouring points. An exponential semi-variogram of the form:  $\gamma(h)=c_0+c_1 [1-\exp(-3 h/a)]$ , where  $h$  is the lag and equals the distance between two intensity points, was adopted for this study in agreement with Ambraseys and Douglas (2004). Ambraseys and Douglas (2004) adopted values of  $c_0=1$ ,  $c_1=1$  and  $a=1000\text{km}$  for this function. The critical parameter is  $a$ , which roughly corresponds to the distance to which an IDP has an influence on the surrounding area. Small values of  $a$  (e.g. 100km) lead to intricate maps where the isoseismals can be jagged as the predicted intensity at a given location is only influenced by close-by observations. Large values of  $a$  (e.g. 1000km) lead to isoseismals with a smooth shape, which is closer to those obtained by manual drawing (e.g. Figure 2).

To determine which  $a$  is best adapted to France, experimental semivariograms were derived for the 109 earthquakes with 100 or more intensity points in the database. To construct these semivariograms a standard procedure was adopted (e.g. Jayaram and Baker, 2009) but with the modification that only intensities at roughly the same epicentral distances were compared (within intervals of 25km). This is to limit the impact of the expected decay in intensities. Distance intervals of 25km were used to construct the experimental semivariograms, although intervals of 10km and 50km were also tried with similar results. Exponential models were fitted by least-squares regression in order to find  $a$ . Most of the experimental semivariograms obtained did not show clear patterns, with  $\gamma(h)$  not showing much dependence on the lag  $h$  (e.g. in the case of the Saint Dié 2003 event, Figure 3a). This implies that close-by intensities are not more inter-correlated than distant observations.

The difficulty of measuring the spatial correlation of IDPs might be due to the narrow range of available intensities (generally for SisFrance database from III to VII) and their discrete nature (i.e. integer values). Also, local effects could add additional variability to the intensity observations, thereby making the experimental semivariogram more variable. Nonetheless,



for some earthquakes, the experimental semivariograms showed the expected behaviour with correlation decreasing with lag (separation between two intensity observations). As an example, in Figure 3b the experimental semi-variogram obtained from the 431 intensity points of the 1972 Ile d'Oléron earthquake is shown (exponential model fitted with  $a=1,979\text{km}$ ).

Finally, the same  $a$  value as Ambraseys and Douglas (2004) was selected ( $a=1000\text{km}$ ) as it provided the best match to the manually drawn maps (Rey *et al.*, 2013). As intensity is a discrete quality, which does not generally show large differences between neighbouring locations,  $a=1000\text{km}$  appears to be an appropriate choice. This is in contrast to correlation models for instrumentally-measured ground-motion parameters (e.g. PGA), for which much smaller values of the parameter  $a$  are justified (e.g. Jayaram and Baker, 2009).

### **Comparison between estimated intensities and PSHAs**

Rather than testing the MEDD2002 PSHA study (Martin *et al.* 2002), used to establish the current French zoning but which relies on models that are now mostly out-dated, we decided to test the latest European seismic hazard results (ESHM13) produced by the SHARE European project (Woessner *et al.*, 2015). Mean hazard values for PGA and elastic response spectral accelerations for selected structural periods are available, based on a logic tree including three alternative source models and a set of ground-motion prediction equations. The mean hazard curves at the twenty-four selected cities in France have been downloaded from the epher.org website (Figure 4). Hazard estimates vary greatly between the cities, ranging from 0.013 (in Paris) to 0.3g (in Lourdes) for PGA and a return period of 475 years.

#### *Preparing the data to enable the comparisons*

Because ESHM13 hazard estimates are in terms of PGAs, intensities must be converted into PGAs to compare the model predictions with the intensity history. The best option would be to use a GMICE based on French data. This would require a large set of co-located PGA and intensity observations from France; a dataset which is not available at present given the low seismicity rates in France. The Caprio *et al.* (2015) global GMICE is used for this purpose here. This equation is used in the ShakeMaps produced by the BCSF because it proved to be rather well adapted for France (Schlupp, 2016).

Determining the time windows of completeness for each intensity level at the 24 sites is a difficult task. Ideally, completeness time periods should be determined using methods that are independent of the intensity datasets, e.g. on historical grounds like Stucchi *et al.* (2013). In France, such a historical analysis is not available, and complete time windows can only be

determined from the intensity data itself. An analysis of the intensity dataset shows that intensity level III is not complete; therefore only intensities higher or equal to IV are considered further. As done classically for determining completeness of earthquake catalogues (e.g. Burkhard and Grunthal 2009; Beauval *et al.* 2013), the complete time window is determined visually from the cumulative number of intensities versus time (Table 1). Stable rates of occurrence over time indicate complete periods. Time windows of completeness are estimated considering intensities higher or equal to IV. These time windows are also used for higher intensity levels, as the datasets for these intensity levels is too restricted to evaluate meaningful time windows. Graphs showing the cumulative number of intensities versus time, for the 24 selected sites, are displayed in the Electronic Supplement. As the identification of the complete time window is associated with large uncertainties, comparison tests are also made using slightly longer and slightly shorter time windows (extension and reduction, respectively, by 50 years), to evaluate the impact on the results.

#### *Summary of the comparison procedure for a given intensity level (e.g. IV)*

1. The history in intensity has been produced at the 24 selected French communities relying on interpolations of the SisFrance database (see section “Construction of a database of interpolated intensities for France”), then for each city;
2. Estimate the complete time window for intensities higher or equal to IV (e.g. 1750-2007 for Clermont-Ferrand, 258 years);
3. Count the number of exceedances of intensity level IV over the complete time window;
4. Convert the intensity IV into PGA using the Caprio *et al.* (2015) global relation. Extract from the ESHM2013 PGA hazard curve the annual exceedance rate corresponding to this PGA. Calculate the expected mean number of exceedances of this PGA over a window with same length as the complete time window (e.g. 258 years for Clermont-Ferrand). Calculate also the number of exceedances corresponding to the percentiles 2.5 and 97.5% assuming a Poisson distribution [for details see, e.g., Tasan *et al.* (2014)];
5. Compare observed and expected numbers of exceedances, corresponding to the same time window (with the same length as the complete time window). Note that we could re-scale the observed number based any length of windows.

#### *Comparisons in terms of number of exceedances*

For a given intensity level, the predicted mean number of exceedances is compared to the observed number of exceedances. The time window considered has the same length as the

time window of completeness for intensity IV, thus this time window varies from one city to the other. For example, for Clermont-Ferrand and an intensity of IV (corresponding to a PGA of 0.011g), the ESHM13 mean annual rate of exceedance is 0.0294. As the time period of completeness is 258 years (1750-2007), the predicted mean number of exceedances of intensity IV over 258 years is  $0.0294 \times 258 = 7.6$  (Figure 5, abbreviation “CFE”). In the probabilistic seismic hazard model, earthquake ground motions are assumed to occur according to a Poisson process, so this number is only a mean value. It is more appropriate to consider an interval and the percentiles 2.5 and 97.5% corresponding to 3 to 13 expected intensities higher or equal to IV (Figure 5). In the case of Clermont-Ferrand, the observed number is within the predicted distribution, with 12 intensities higher or equal to IV “observed” during the period 1750-2007.

Figure 5 displays the comparison between predicted and observed exceedance numbers for intensity IV at the 24 selected cities. The order of the cities, from left to right, corresponds to increasing hazard estimated by ESHM13 (increasing annual exceedance rate for intensity IV). For half of the cities (12 out of 24 cities), the observation is within the predicted range, i.e. within the percentiles 2.5 and 97.5% (e.g. Rennes, Lille, Aix-en-Provence and Avignon). For the other half, the observed numbers are larger than predicted. The sites where the observed number is much higher than predicted are distributed all over France, in the west (e.g. Le Havre and Bordeaux), in the south-west (Lourdes), and in the east (Grenoble, Chambéry, Annecy and Strasbourg). Lourdes is where the discrepancy between predicted and observed number is the largest, with 7 to 22 intensities expected over 1850-2007, compared to 53 observed.

As the determination of completeness time windows is associated with large uncertainties, the comparison is repeated considering slightly longer or slightly shorter complete time windows. Extending the window back in time by 50 years, or shortening this window by 50 years, leads to results that are not that different: 14 out of 24 cities with observations within the predicted range when extending the window, 15 out of 24 cities when shortening the window (results not shown).

The analysis for intensity level V leads to comparable results (Figure 6), but with lower expected numbers of exceedance. 14 cities out of 24 have experienced a number of exceedances within the expected range. In Clermont-Ferrand, for example, up to 5 intensities higher or equal to V are expected over a time window of 258 years (97.5<sup>th</sup> percentile), whereas 3 have been observed (between 1750 and 2007). Ten out of 24 sites have experienced a number of exceedances larger than the predicted percentile 97.5%. This is the case, for example, for Bordeaux, Besançon, Grenoble, Chambéry and Annecy.

The results for intensity level VI are less clear (Figure 7), there are few available data and the observed numbers of exceedances are small over the considered periods. The time windows considered are too short with respect to the return periods of such levels. Nonetheless, for 7 out of 8 cities with observed numbers larger than zero (Bordeaux, Lille, Grenoble, Chambéry, Nice, Strasbourg, Lourdes), observations are within the range of predictions (the exception is Annecy).

Throughout this article, mean hazard estimates are considered in the comparison with observations. However, as with any state-of-the-art PSHA study, ESHM13 results are expressed in terms of mean and percentile hazard curves, resulting from the exploration of a source model logic tree as well as a ground-motion model logic tree (Woessner *et al.* 2015; note that this percentile has no relation with the percentile associated with the Poisson distribution). As expected, comparisons are different if considering other hazard estimates than the mean. For example, if the 85<sup>th</sup> percentile (taken from the epher.org website) is considered, predicted exceedance numbers increase, and all but three cities show an agreement between observations and predictions (Figure 8).

#### *Taking into account the uncertainty associated to the GMICE in the comparison*

The uncertainty in the conversion from intensity to PGA using the GMICE is significant. For a given intensity, Caprio *et al.* (2015) associates a standard deviation of 0.4 to the predicted logarithm of the mean PGA. To check how much this uncertainty impacts the results, the normal distribution modelled by the Caprio *et al.* (2015) GMICE is sampled and 10,000 synthetic PGA datasets are generated from the original intensity dataset, at a location. An example dataset is displayed in Figure 9 for Clermont-Ferrand. Including the uncertainty on the conversion from intensity to PGA, a distribution for the observed number of exceedances over the time period of completeness is obtained.

Figure 10 compares the number of exceedances predicted by ESHM13 in Lourdes over a time window of 158 years, for accelerations between 0.001g and 1g, with the observed distribution including the uncertainty on the intensity-PGA conversion (counted over the time window of completeness 1850-2007). Intensity levels IV, V and VI are considered. Again, observations are larger than predicted by the model for accelerations of 0.011g and 0.046g (intensities IV and V). At 0.084g (intensity VI), the predicted and the observed distributions are slightly overlapping. The results for intensity VI should be considered with care; there are few intensity observations greater than or equal to VI and the time windows considered are short with respect to the return periods of such intensities. Including the uncertainty in the intensity-PGA conversion does not change the overall results. For Clermont-Ferrand, for

example, observations and predictions agree rather well, with means of observed distributions within the predicted range (percentiles 2.5 and 97.5%, Figure 11). For Nancy, observations are above predictions for acceleration levels of 0.011g and 0.046g (Figure 12), which is in agreement with Figure 5.

## Conclusions

An inventory of macroseismic intensities at the municipal level was created in this study for the first time for mainland France. This database was produced via a robust interpolation technique from an existing well-established database of intensities of historical earthquakes (SisFrance). The intensity history is thus obtained for 24 French cities distributed over the whole country in various seismotectonic contexts. These interpolated intensities were compared with the history expected from the recent probabilistic seismic hazard assessment for Europe (ESHM13) produced by the SHARE project. The benefit of using macroseismic intensities for this comparison is that it extends the time period available for this comparison to centuries rather than decades, which is the case for instrumental records. This is particularly important for an area of low to moderate seismicity, such as mainland France. This advantage in the temporal domain (as well as increased spatial coverage with respect to instrumental networks), however, needs to be weighed against disadvantages concerning uncertainties from: the original estimation of macroseismic intensities from historical documents; problems in interpolation due to, e.g., lack of data and offshore epicentres; assessment of completeness time periods; and the conversion between intensity and peak ground acceleration.

We find that exceedance rates estimated in ESHM13 (mean model) are in agreement with the observations (intensity IV and V, corresponding to moderate shaking) for approximately half of the sites considered. For the other sites, the estimated exceedance rates are lower than the observations. The comparison is also made for intensity level VI, which shows a better match; however, great caution must be taken for this intensity as few data are available. A reason for predicting lower intensities than observed could be related to the minimum moment magnitude 4.5 used for ESHM13 (Woessner *et al.*, 2015). Magnitudes lower than 4.5 do not contribute to the hazard estimated although they can produce intensities higher or equal to IV close to the epicentre. Another reason for the discrepancy could be due to epistemic uncertainty in the choice of the equation to convert intensities to peak ground acceleration and also the uncertainty inherent in making such a conversion. Finally, the hazard calculations in ESHM13 are for average 'rock' conditions, whereas the interpolated intensities inevitably include local site effects that may amplify ground motions (Bossu *et al.*, 2000).

The database of the interpolated intensities also includes the municipalities of French overseas territories (Rey *et al.*, 2015b). The same type of comparison could also be undertaken for these locations but it will be even more challenging as the historical catalogue is shorter (rough 200 years) and it includes many offshore epicenters.

The Matlab script used for kriging is freely available on request from the corresponding author. The database is available as a French web-service for geological risks: <http://www.georisques.gouv.fr/dossiers/seismes/donnees#/> (last accessed October 2017).

## **Acknowledgements**

We thank Daniel Monfort-Climent, Philippe Daniels, Sindy Raout, Samuel Auclair, Pierre Gehl and, particularly, Jérôme Lambert for their contributions to the project on the creation of the database of interpolated intensities, which was funded by the French Ministry of the Environment. Early versions of this study were presented at the 35<sup>th</sup> General Assembly of the European Seismological Commission, the 9<sup>th</sup> National Colloquium of the French Association of Earthquake Engineering (AFPS2015) and the 4<sup>th</sup> International Colloquium on Historical Earthquakes and Macroseismology. We thank those people who commented on these presentations. Finally, we thank two anonymous reviewers for their comments on the first version of this article.

## **References**

- Ambraseys, N. N. and Douglas, J. (2004), Magnitude calibration of north Indian earthquakes, *Geophysical Journal International*, **159**, 165–206.
- Bakun, W.H. and O. Scotti (2006), Regional intensity attenuation models for France and the estimation of magnitude and location of historical earthquakes. *Geophysical Journal International*, **164**, 596-610.
- Beauval, C., Bard, P.-Y., Hainzl, S. and Guéguen, P. (2008), Can strong-motion observations be used to constrain probabilistic seismic hazard estimates?, *Bulletin of the Seismological Society of America*, **98**, 509-520.
- Beauval C. (2011), On the use of observations for constraining probabilistic seismic hazard estimates-brief review of existing methods, *Applications of Statistics and Probability in Civil Engineering*, Faber, Kohler and Nishijima editors, London, 763-767 (ISBN 978-0-415-66986-3).
- Beauval, C., H. Yepes, P. Palacios, M. Segovia, A. Alvarado, Y. Font, J. Aguilar, L. Troncoso, and S. Vaca (2013), An earthquake catalog for seismic hazard assessment in

Ecuador, *Bulletin of the Seismological Society of America*, **103**, 773–786, doi: 10.1785/0120120270.

Bossu, R., Scotti, O., Cotton, F., Cushing, M. and Levret, A. (2000), Determination of geomechanical site effects in France from macroseismic intensities and reliability of macroseismic magnitude of historical events. *Tectonophysics*, **324**, (1–2), 81–110.

BRGM/EDF/IRSN (2017), Base de données SISFRANCE – [www.sisfrance.net](http://www.sisfrance.net), Last accessed April 2017.

Burkhard M. and G. Grunthal (2009), Seismic source zone characterization for the seismic hazard assessment project PEGASOS by the Expert Group 2 (EG1b), *Swiss Journal of Geosciences*, **102**, 149-188, DOI 10.1007/s00015-009-1307-3.

Caprio, M., Tarigan, B., Worden, C. B., Wiemer, S. and Wald, D. J. (2015), Ground motion to intensity conversion equations (GMICEs): A global relationship and evaluation of regional dependency, *Bulletin of the Seismological Society of America*, **105**(3), 1476-1490, doi: 10.1785/0120140286.

Council of Europe (1998), European macroseismic scale 1998 (EMS-98), Grünthal G (ed.), vol. 15, Centre Européen du Géodynamique et de Séismologie: Luxembourg.

Douglas, J. (2017), Ground motion prediction equations 1964–2017, <http://www.gmpe.org.uk>. Last accessed October 2017.

Jayaram, N. and Baker, J. W. (2009), Correlation model for spatially distributed ground-motion intensities, *Earthquake Engineering and Structural Dynamics*, **38**, 1687-1708, doi: 10.1002/eqe.922.

Lambert, J. (2004), Base de données SisFrance et SisFrance-Antilles, Sites internet, année 2004. Rapport final. Rapport BRGM/RP-53333-FR, 33 pp. In French.

Mak, S. and Schorlemmer, D. (2016), A Comparison between the Forecast by the United States National Seismic Hazard Maps with Recent Ground-Motion Records, *Bulletin of the Seismological Society of America*, **106**(4), 1817-1831.

Manchuel, K., Traversa, P., Baumont, D., Cara, M, Nayman, E., Durouchoux, C., (2017), The French seismic CATalogue (FCAT-17), *Bulletin of Earthquake Engineering*, doi: 10.1007/s10518-017-0236-1.

Martin, C., Combes, P., Secanell, R., Lignon, G., Carbon, D., Fioravanti, A. & Grellet, B., 2002. Révision du zonage sismique de la France: étude probabiliste, under the supervision

of the Groupe d'Etude et de Proposition pour la Prévention du risque sismique en France and the Association Française du Génie Parasismique (in French), Geoter Report, GTR/MATE/0701-150.

Medvedev, S. P., Sponheuer, W. and Karnik, V. (1967), Seismic intensity scale version 1964. *Inst. Geody. Publ.*, Jena, 48 pp.

Mucciarelli, M., Albarello, D. and D'Amico, V., (2008), Comparison of probabilistic seismic hazard estimates in Italy, *Bulletin of the Seismological Society of America*, **98**, 2652–2664.

Musson, R. M. W. (2000), Intensity-based seismic risk assessment, *Soil Dynamics and Earthquake Engineering*, **20**(5-8), 353-360. doi: 10.1016/S0267-7261(00)00083-X.

Musson R.M.W., Grünthal G., Stucchi, M. (2010). The comparison of macroseismic intensity scales. *Journal of Seismology*, **14** (2), pp.413-428.

Olea, R. A. (1999), *Geostatistics for engineers and earth scientists*, Kluwer Academic Publishers, Dordrecht.

Rey, J., Auclair, S., Douglas, J. and Lambert, J. (2013), Faisabilité et test d'une base de données des intensités macrosismiques historiques extrapolées pour les communes métropolitaines (phase 1), Final report. BRGM/RP-62941-FR, 75 p., 40 fig., 2 tabl., 1 ann. In French.

Rey, J., Auclair, S. and Monfort Climent, D. (2015a), Etablissement d'une base de données des intensités historiques extrapolées pour toutes les communes françaises (phase 2), Final report, BRGM/RP-64384-FR, 52 p., 11 fig., 4 tabl., 2 ann. In French.

Rey, J., Auclair, S., Daniels, P., Monfort Climent, D. and Raout, S. (2015b), Etablissement d'une base de données des intensités historiques extrapolées pour toutes les communes françaises (phase 3), Final report, BRGM/RP-65304-FR, 39 p., 2 ann. In French.

Schlupp, A. (2016), ShakeMap fed by macroseismic data in France: feedbacks and contribution for improving SHA, AGU Fall Meeting, December 12-16, San Francisco.

Scotti, O., Baumont, D., Quenet, G. and Levret, A. (2004), The French macroseismic database SISFRANCE: objectives, results and perspectives, *Annals of Geophysics*, **47**(2/3).

Stirling, M. and Petersen, M. (2006), Comparison of the Historical record of earthquake hazard with seismic-hazard models for New Zealand and the Continental United States, *Bulletin of the Seismological Society of America*, **96**, 1978–1994.



Stucchi, M., Rovida, A., Gomez Capera, A.A. *et al.* (2013), The SHARE European Earthquake Catalogue (SHEEC) 1000–1899, *Journal of Seismology*, **17**(2), 523–544. doi:10.1007/s10950-012-9335-2.

Tasan, H., Beauval, C., Helmstetter, A., Sandikkaya, A. and Guéguen, P. (2014), Testing probabilistic seismic hazard estimates against accelerometric data in two countries: France and Turkey, *Geophysical Journal International*, **198**(3), 1554-1571.

Woessner, J., Laurentiu, D., Giardini, D. *et al.* (2015), The 2013 European Seismic Hazard Model: Key components and results, *Bulletin of Earthquake Engineering*, **13**(12), 3553-3596, doi: 10.1007/s10518-015-9795-1.

## Tables

<b>Municipality</b>	<b>Abbreviation</b>	<b>Time window (level IV and V)</b>	<b>Number of IDPs &gt;= level IV</b>	<b>Number of IDPs &gt;= level V</b>	<b>Number of IDPs &gt;= level VI</b>
<b>Aix-en-Provence</b>	AIX	1800-2007	19	9	1
<b>Ajaccio</b>	AJA	1750-2007	3	0	1
<b>Annecy</b>	ANN	1750-2007	44	15	12
<b>Avignon</b>	AVI	1650-2007	23	9	1
<b>Besançon</b>	BES	1575-2007	37	13	1
<b>Bordeaux</b>	BDX	1620-2007	13	9	2
<b>Chambéry</b>	CHA	1750-2007	26	17	9
<b>Clermont- Ferrand</b>	CFE	1750-2007	19	6	3
<b>Dijon</b>	DIJ	1550-2007	28	7	0
<b>Grenoble</b>	GRE	1750-2007	27	22	4
<b>Le Havre</b>	HAV	1550-2007	17	4	1
<b>Lille</b>	LIL	1350-2007	11	4	4
<b>Lourdes</b>	LDE	1850-2007	54	27	12
<b>Marseille</b>	MRS	1850-2007	20	7	0
<b>Montpellier</b>	MPL	1750-2007	19	4	0
<b>Nancy</b>	NCY	1550-2007	24	6	2
<b>Nantes</b>	NTE	1750-2007	29	2	1
<b>Nice</b>	NCE	1800-2007	25	10	7
<b>Paris</b>	PAR	1350-2007	11	1	0
<b>Perpignan</b>	PER	1750-2007	23	12	3
<b>Rennes</b>	RNS	1750-2007	24	6	0
<b>Saint-Etienne</b>	STE	1750-2007	26	8	0
<b>Strasbourg</b>	SXB	1550-2007	42	23	5
<b>Toulouse</b>	TLS	1620-2007	18	6	3

**Table 1:** Time window of completeness for intensity levels IV, extended to levels V and VI, and number of IDPs within this time windows for the 24 municipalities of the study.

## Figures

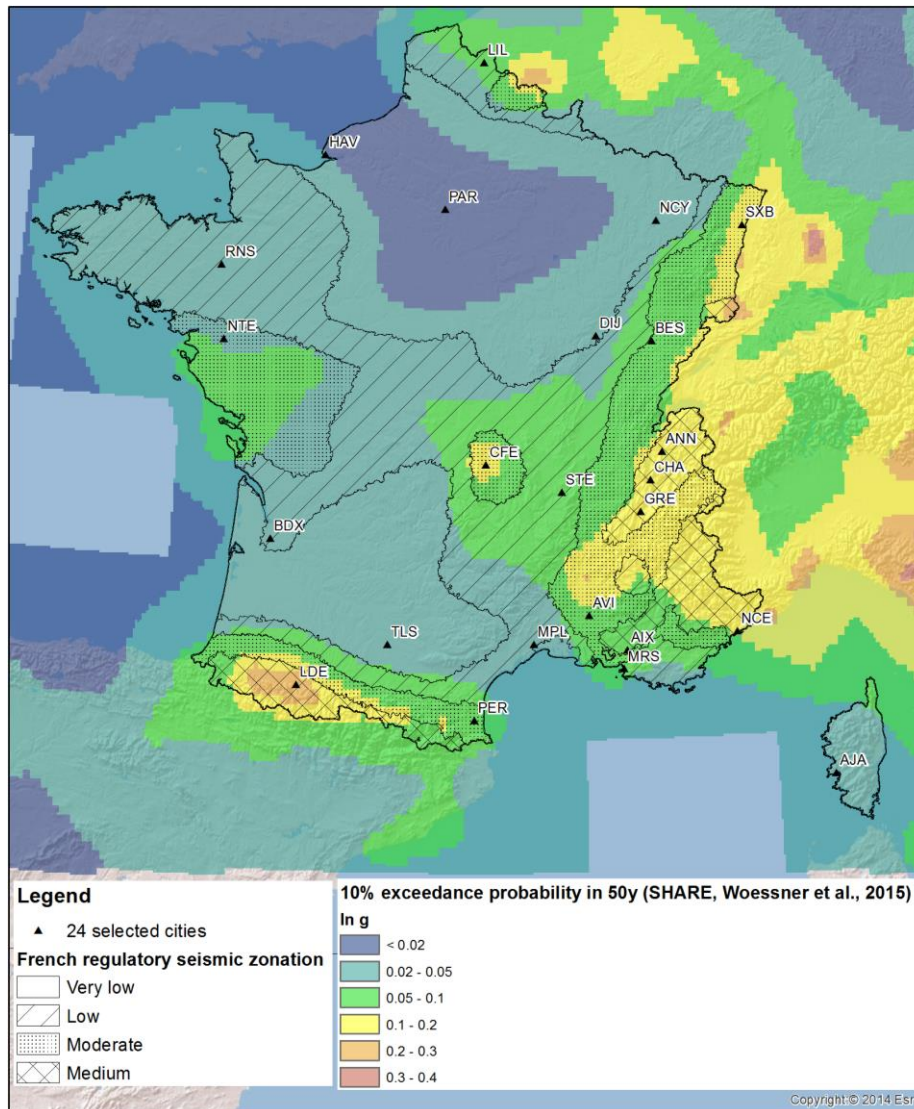


**Figure 1:** Peak Ground Accelerations with 10% exceedance probability in 50 years predicted by the mean ESHM13 ([www.efher.org](http://www.efher.org), Woessner *et al.*, 2015), and the twenty-four selected municipalities representative of the four zones of the French regulatory seismic zonation. AIX : Aix-en-Provence; AJA : Ajaccio ; ANN : Annecy ; AVI : Avignon ; BDX : Bordeaux ; BES : Besançon ; CHA : Chambéry ; CFE : Clermont-Ferrand ; DIJ : Dijon ; GRE : Grenoble ; HAV : Le Havre ; LDE : Lourdes ; LIL : Lille ; MPL : Montpellier ; MRS : Marseille ; NCE : Nice ; NCY : Nancy ; NTE : Nantes ; PAR : Paris ; PER : Perpignan ; RNS : Rennes ; STE : Saint-Etienne ; SXB : Strasbourg ; TLS : Toulouse.

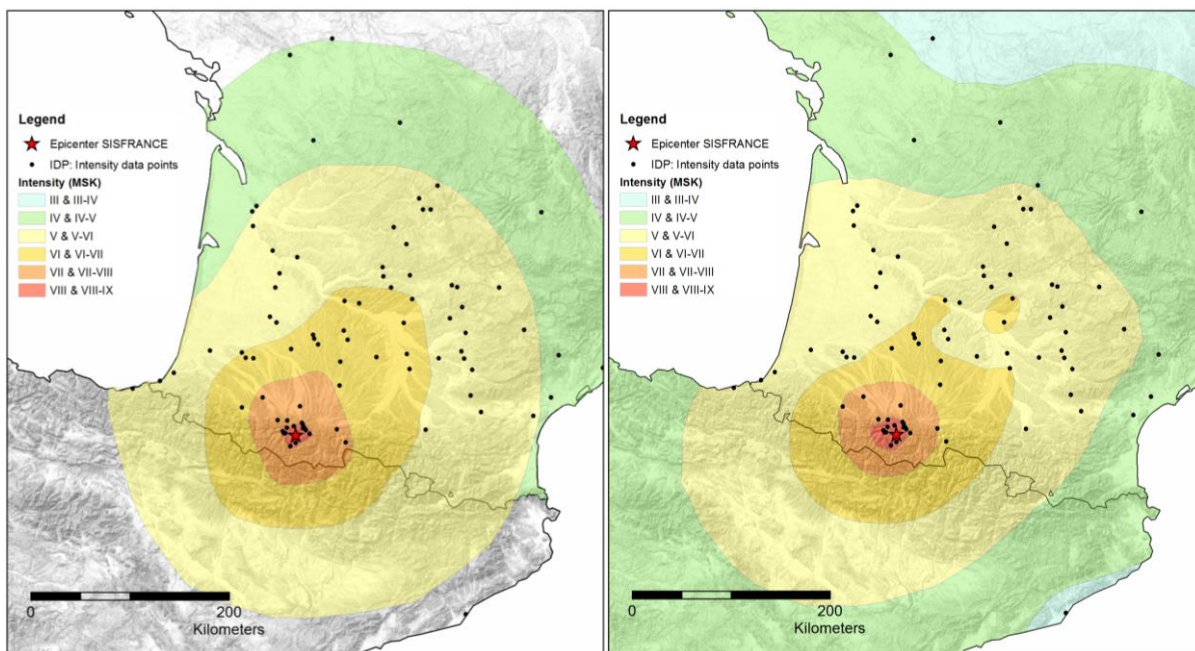
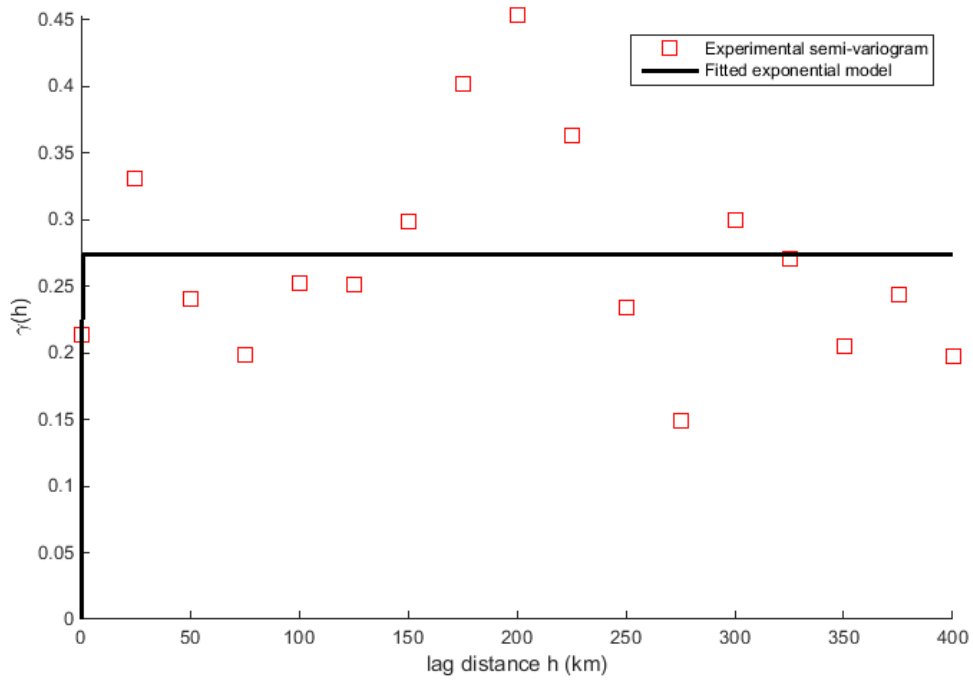


**Figure 2:** Isoseismal maps for the 21 June 1660 Bigorre earthquake drawn manually (left, from Lambert, 2004) and using the kriging approach (right, this study).

(a)



(b)

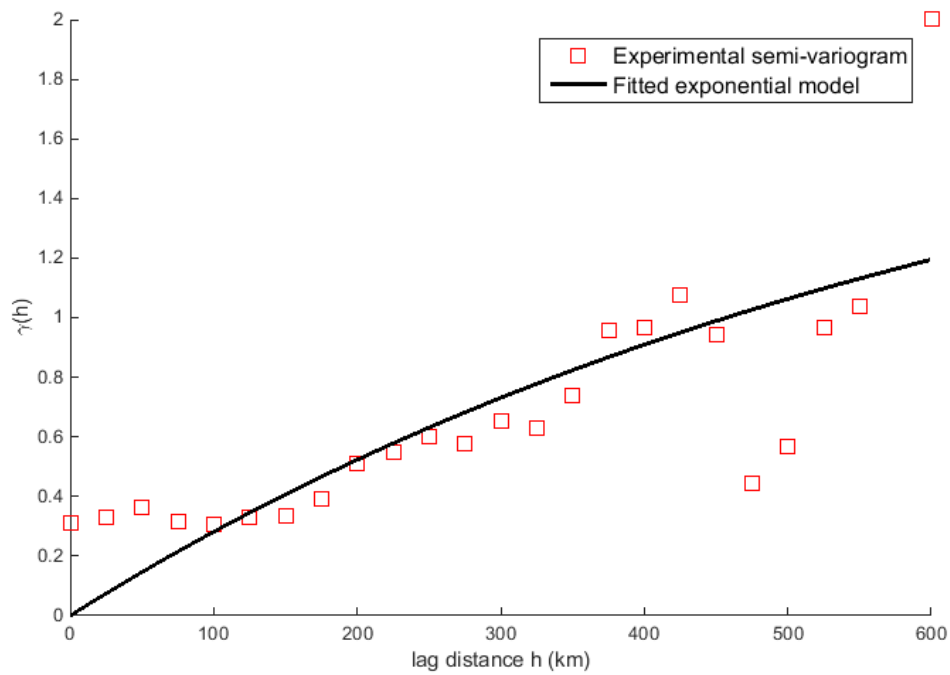


**Figure 3:** Experimental semi-variogram and the fitted exponential model for the (a) 22 February 2003 St Dié and (b) 7 September 1972 Ile d'Oléron earthquakes.

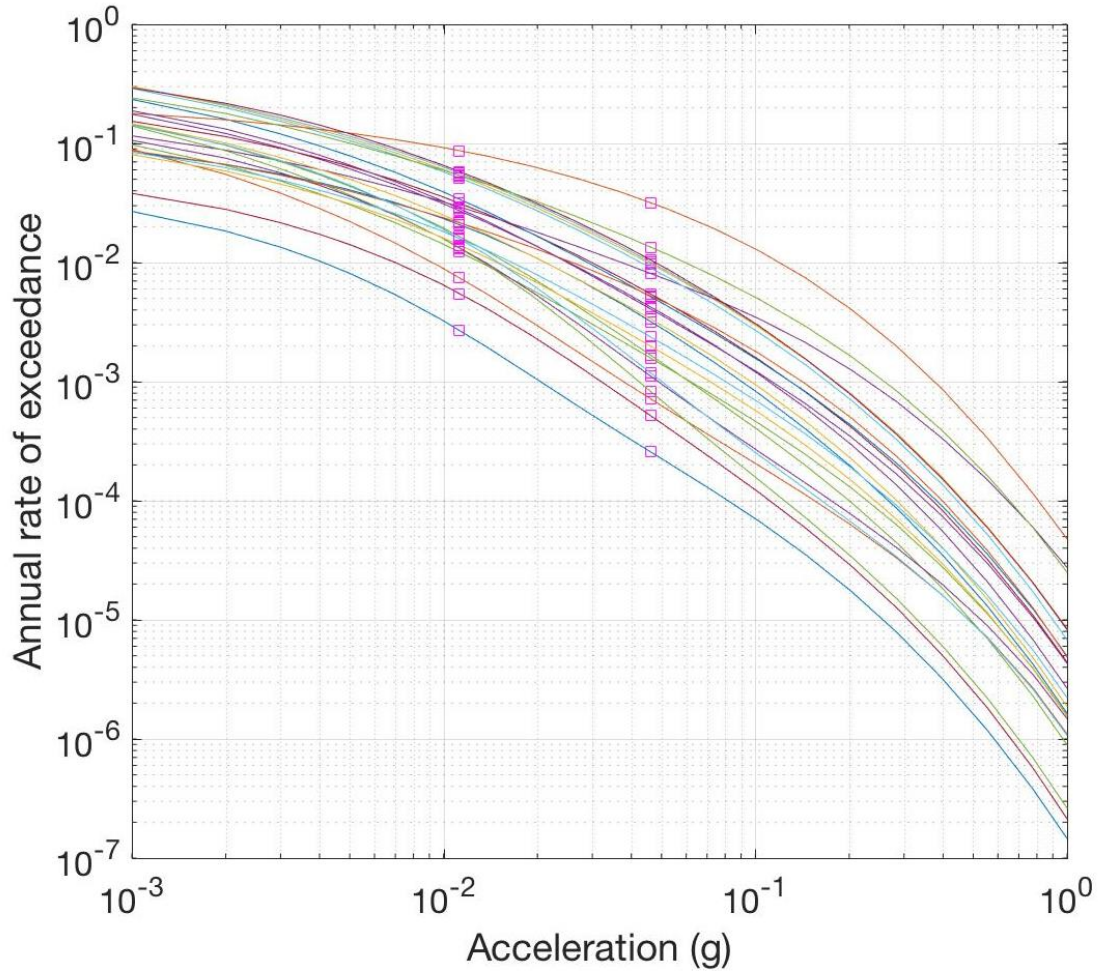


**Figure 4:** ESHM13 mean hazard curves (PGA, rock), obtained from epher.org. Pink squares indicate the rates interpolated for intensity IV (0.011g) and intensity V (0.046g, Caprio *et al.* 2015). Accelerations for 10% exceedance probability over 50 years (0.0021 annual rate) vary from 0.013g to 0.3g depending on the municipality.

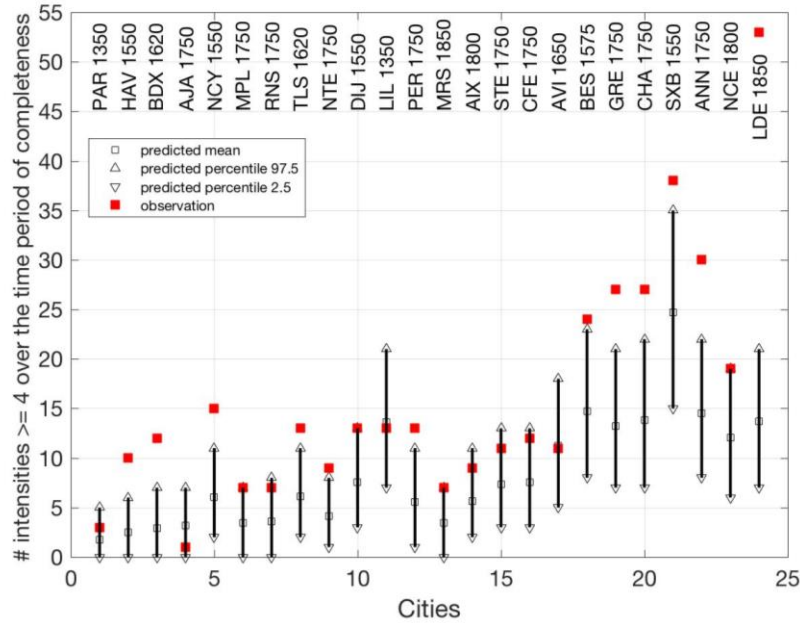


**Figure 5:** Comparison of predicted number of exceedances with “observed” number, for intensity level IV at 24 cities (equivalent to PGA 0.011g, Caprio *et al.* 2015). For each city, the time window considered has the same length as the time window of completeness for intensity IV. Mean exceedance number obtained from the mean SHARE annual exceedance rate; percentiles account for the variability of the number over the time window (Poisson distribution). Beginning date of complete time window indicated after the acronym of the city. See legend of Fig. 1 for acronyms. Cities are ordered, from left to right, according to increasing hazard as estimated by ESHM13 (increasing annual exceedance rate for PGA 0.011g).

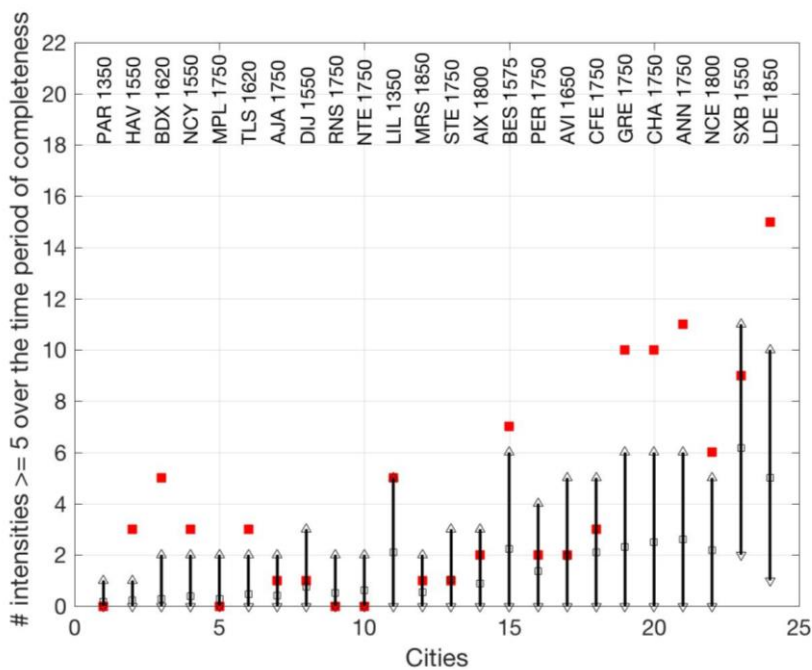


**Figure 6:** Comparison of predicted number of exceedances with “observed” number, for intensity level V at 24 cities (equivalent to PGA 0.046g, Caprio *et al.* 2015). Beginning date of complete time window indicated after the acronym of the city. Cities are ordered, from left to right, according to increasing hazard as estimated by ESHM13 (increasing annual exceedance rate for PGA 0.046g). See legend of Figure 6.

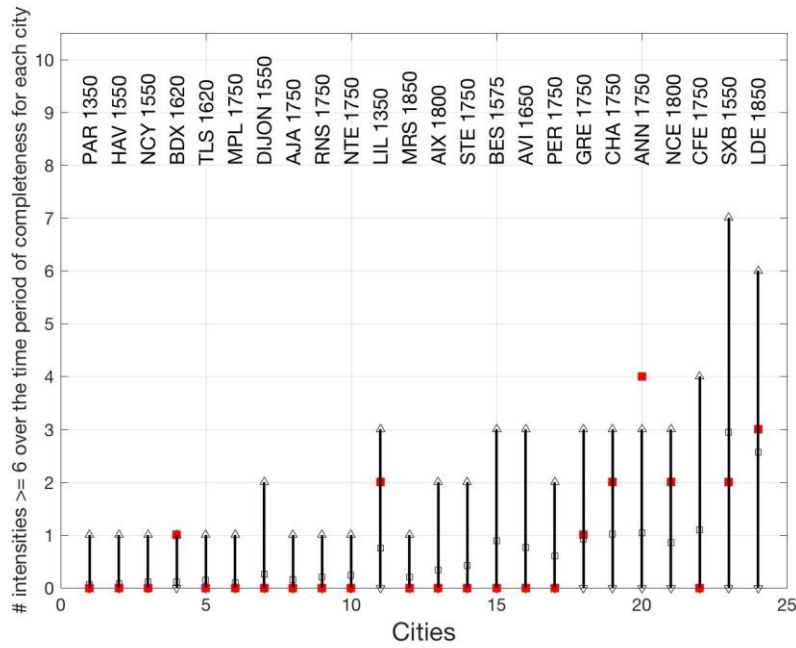


**Figure 7:** Comparison of predicted number of exceedances with “observed” number, for intensity level VI at 24 cities (equivalent to PGA 0.084g, Caprio *et al.* 2015). Beginning date of complete time window indicated after the acronym of the city. Cities are ordered, from left to right, according to increasing hazard as estimated by ESHM13 (increasing annual exceedance rate for PGA 0.084g). See legend of Figure 6.

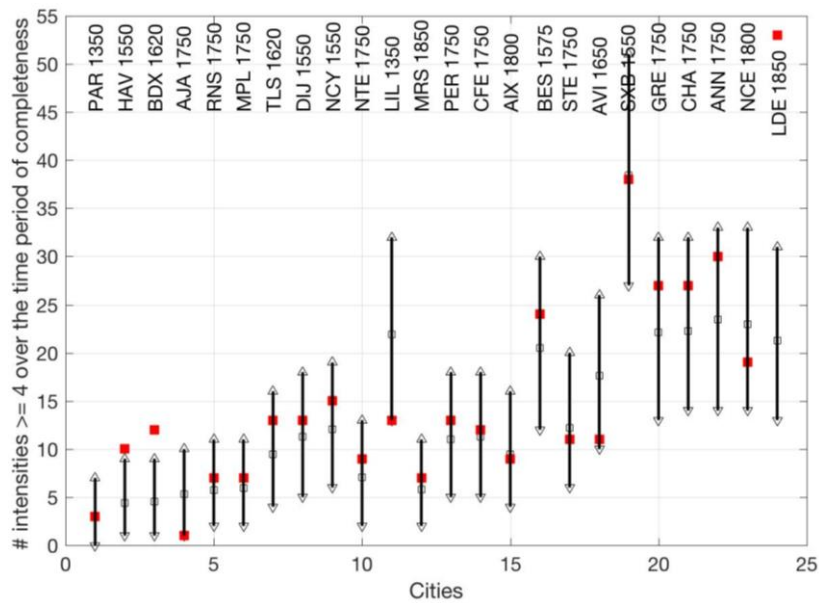


**Figure 8:** Comparison of predicted number of exceedances with “observed” number, for intensity level IV at 24 cities (PGA 0.046g). The difference with Figure 5 is that instead of using the mean annual rate of exceedance provided by SHARE relying on the logic tree calculations (efher.org), the percentile 85% is used. See also legend of Figure 6.



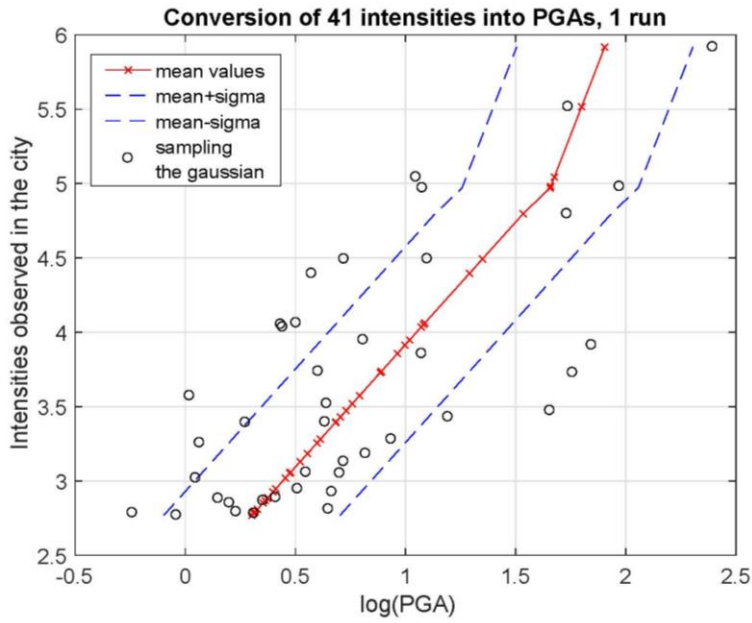


**Figure 9:** Example of one synthetic PGA dataset generated from the observed intensities within the time window of completeness, in Clermont-Ferrand. Sampling the Gaussian distributions predicted by Caprio *et al.* (2015), 10,000 synthetic datasets like this one are generated.

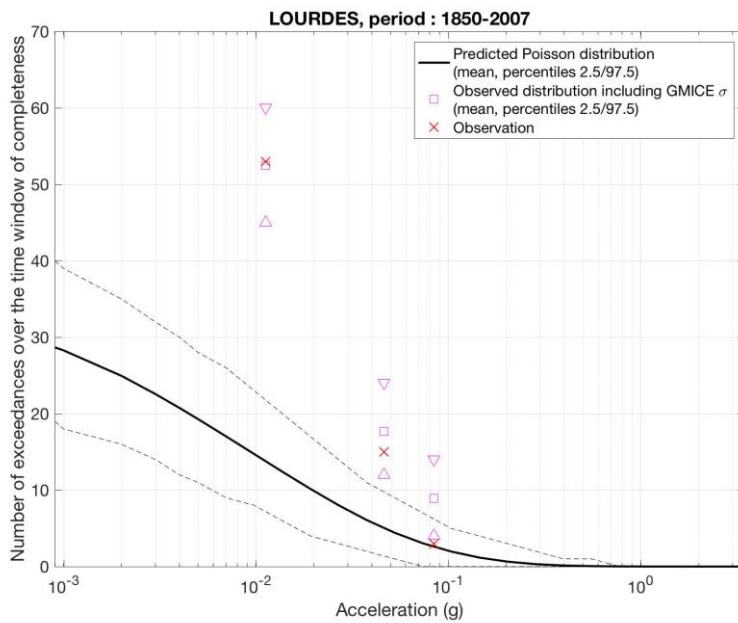


**Figure 10 :** Lourdes, comparison of predicted number of exceedances with observed number, for three intensity levels: IV (0.011g), V (0.046g), VI (0.084g, Caprio *et al.* 2015). The time window considered is the time window of completeness (1850-2007). Predicted Poisson distribution obtained from the mean annual rate estimated in SHARE. The uncertainty on the intensity-acceleration equation is taken into account by means of 10,000 synthetic PGA datasets, with intensities converted in PGAs by sampling the normal distribution predicted by Caprio *et al.* (2015, global equation).

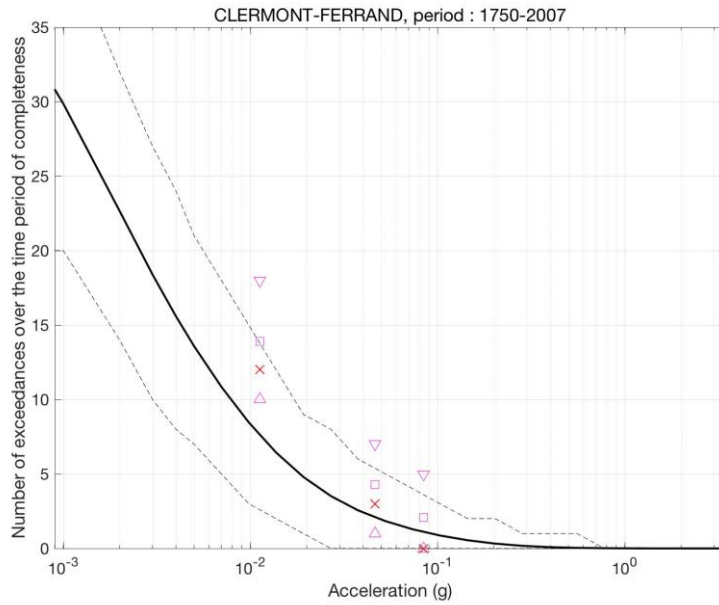


**Figure 11 :** Clermont-Ferrand, comparison of predicted number of exceedances with observed number, for three intensity levels: IV (0.011g), V (0.046g) and VI (0.084g). The time window considered is the time window of completeness (1750-2007). See legend of Figure 10.

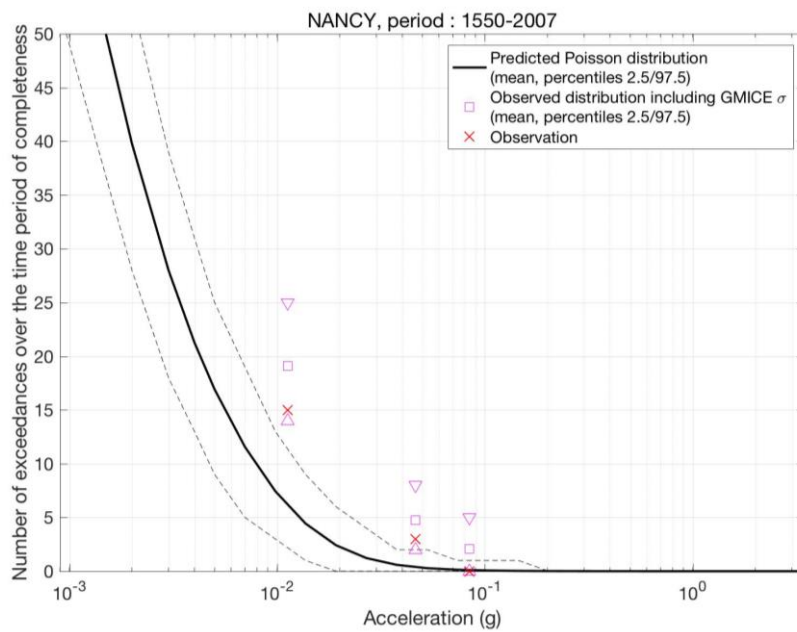


**Figure 12 :** Nancy, comparison of predicted number of exceedances with observed number, for three intensity levels: IV (0.011g), V (0.046g) and VI (0.084g). The time window considered is the time window of completeness (1550-2007). See legend of Figure 10.